Analysis of PLT and CPT by oedo-triaxial model

Analyse des essais PLT et CPT par un modèle oedo-triaxial

G.X.ZHANG, Beijing Geotechnical Institute, Beijing, People's Republic of China
N.R.ZHANG, Beijing Geotechnical Institute, Beijing, People's Republic of China
F.L.ZHANG, Beijing Geotechnical Institute, Beijing, People's Republic of China

SYNOPSIS: A pseudo-elastic model based upon conventional oedometer and triaxial compression tests modified by dynamic triaxial and in situ shear wave velocity tests is developed to simulate the predominantly undrained stress-strain behavior of a medium to dense saturated silty clay of quaternary fluvial-alluvial origin above water table during plate-load and cone-penetration tests. An axial symmetrical finite element program specially adapted to take care of tensile cracks and equipped with strain-controlled dynamic interface elements is developed for the analysis. Promising results are obtained from preliminary analyses and a hitherto unnoticed zone of tensile cracks and plastic flow is shown by the analysis to exist beneath and around the loaded plate isolating a cone-shaped volume of soil under the loaded plate which is the cause of the turning point and the subsequent steep and fairly straight tangent of the load-settlement curve of the plate-load test.

1 INTRODUCTION

Despite the development of high-speed digital computers and finite element methods, a full stress-strain analysis of two of the commonly employed in situ geotechnical tests, the plate-load test (PLT) and the cone-penetration test (CPT) has been slow to appear due to the difficulties in realistic modelling of soil behavior and the complexity of the deformation process (Andersen et al. 1982; Baligh 1985; Battaglio, Bruzzi, Jamiolkowski, and Lancellotta 1986). This paper is a preliminary result of an exploratory effort to analyse the predominantly undrained stress-strain behavior of a medium to dense quaternary clay during these tests with the aim to provide basic information for better interpretation of these tests and to serve as a basis for further improvements such as a complete analysis of CPT with pore-pressure and side-friction predictions, etc.

2 THE MODIFIED OEDO-TRIAXIAL MODEL

A 3-d pseudo-elastic model following the general ideas of Janbu (1977) and similar to the K-G model (Domaschuk et al. 1975) but based upon conventional oedometer and triaxial compression tests modified by dynamic triaxial and in situ shear wave velocity tests done in parallel is developed from an original 1-d consolidation-shear model (Zhang et al. 1981, 1984) that had been applied to settlement analysis in Beijing over the years. Assuming the soil to be isotropic and susceptible to total stress analysis, the constitutive relationship may be written as:

$$\epsilon_i = \frac{\sigma_i+\sigma_j+\sigma_k}{3M_1} + \frac{\sigma_i-\sigma_j}{3M_2}(1+\nu)(1\pm\xi) + \frac{\sigma_i-\sigma_k}{3M_2}(1+\nu)(1\pm\xi) \quad (1)$$

where ϵ_i is the principle strain along direction i; σ_i, σ_j, σ_k are the principle stresses; M_1, M_2 are the tangential volumetric and deviatoric moduli; ν is the Poisson's ratio without volume change and ξ is the coefficient of dilatation defined as positive for contraction, with the sign before it taken as positive when the term $(\sigma_i-\sigma_j)$ or $(\sigma_i-\sigma_k)$ is positive (Fig. 1). The tangential volumetric modulus is obtained from the secant modulus thru differentiation and can be expressed as:

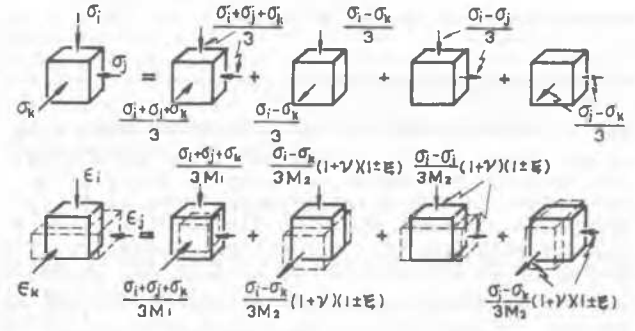

Figure 1. Constitutive relationship

$$M_1 = M_{1s}\frac{\sigma_o+\frac{\Delta\sigma}{2}}{\sigma_o+\frac{\Delta\sigma}{2}(1-b_1)} \quad (2)$$

where M_{1s} is the secant volumetric modulus obtained from regression of oedometer test data; σ_o and $\Delta\sigma$ are the octahedral normal stresses of the natural overburden stresses and the net increase; b_1 is the exponential coefficient of the secant modulus obtained from regression. The tangential deviatoric modulus is obtained from the secant modulus thru differentiation and expressed as:

$$M_2 = M_{2s}(1+b_2) \quad (3)$$

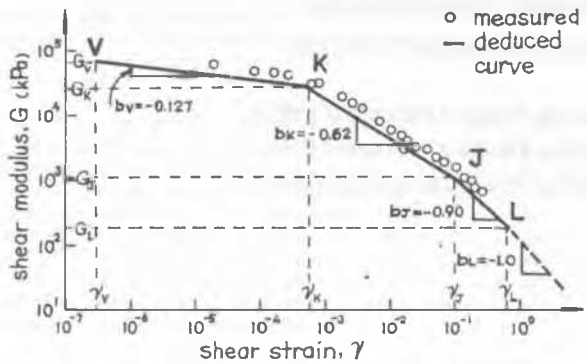

Figure 2. Multi-linear log-log relationship between secant shear modulus and strain

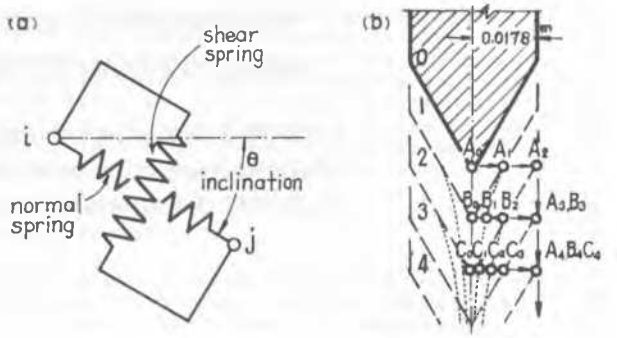

Figure 4. Schematic diagram of strain-controlled dynamic interface element (a)dynamic interface element (modified after Ozawa and Duncan 1973) (b)prescribed step-wise motion of node i

where M_{2s} is the secant deviatoric modulus obtained from regression of CIU triaxial compression, dynamic triaxial and in situ shear wave velocity test data; b_2 is the log decrement ratio of the multi-linear G-γ curve on a log-log plot (Fig. 2). The ν and ξ values are determined by CIU triaxial compression tests with volume change measurements (Zhang et al. 1985).

3 THE STRESS-STRAIN MATRIX

The principle-stress principle-strain matrix D_1 of the above model is obtained from solving Eq. (1). Due to the plus-minus sign in front of ξ determined by the relative magnitudes of the 3 principle stresses and also the possibilities of tensile cracking in 3 directions, there are altogether 16 different ways of writing the D_1 matrix but due to space limit only the case of $\sigma'_r > \sigma'_z > \sigma_t$ without cracks can be given here as follows:

$$D_1 = \begin{bmatrix} \frac{3}{B(3+\xi)} - \frac{C_1}{A} & \frac{1+C_1+C_2}{A} - \frac{3}{B(3+\xi)} & -\frac{C_2}{A} & 0 \\ -\frac{C_1}{A} & \frac{1+C_1+C_2}{A} & -\frac{C_2}{A} & 0 \\ -\frac{C_1}{A} & \frac{1+C_1+C_2}{A} - \frac{3}{B(3-\xi)} & \frac{3}{B(3-\xi)} - \frac{C_2}{A} & 0 \\ 0 & 0 & 0 & \frac{1}{2B} \end{bmatrix} \quad (4)$$

where $A = \frac{1}{M_1}$; $B = \frac{1+\nu}{M_2}$; $C_1 = \frac{A-B(1-\xi)}{B(3+\xi)}$; $C_2 = \frac{A-B(1+\xi)}{B(3-\xi)}$.

Since tensile cracks occur on principle planes where the allowable tensile stresses are exceeded, the D_1 matrix is obtained when this happens by filling zeros into the corresponding row or rows. The stress-strain matrix D is obtained from D_1 thru a transformation matrix T (see e.g. Zienkiewicz 1971) as shown in Fig. 3:

$$D = [T][D_1][T]^T. \quad (5)$$

The residual stresses on the cracked planes are reduced to zero and transformed into additional loads on corresponding nodes for the next iteration.

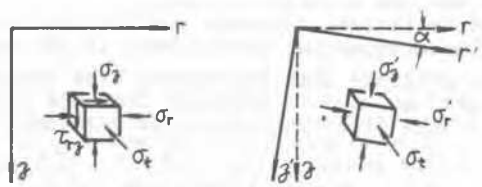

Figure 3. Rotation of principle axes

4 STRAIN-CONTROLLED DYNAMIC INTERFACE ELEMENT

Double-spring interface elements as proposed by Ozawa and Duncan in 1973 are implemented on the border between the soil and its adjacent material (Fig.4a) but are made to move on one end if necessary according to prescribed step-wise motion to simulate the process of penetration (Fig.4b). The angle of inclination and the area of contact are made to change in collaboration with the motion and since the spring-constants are given as kPa per unit displacement per unit area, they also change with the motion. In order to keep sliding on the surface of the cone during penetration, the forces in the normal and shear springs of an interface element in contact with the cone must also satisfy the condition of plastic equilibrium.

5 CALIBRATION THRU A TRIAXIAL COMPRESSION TEST

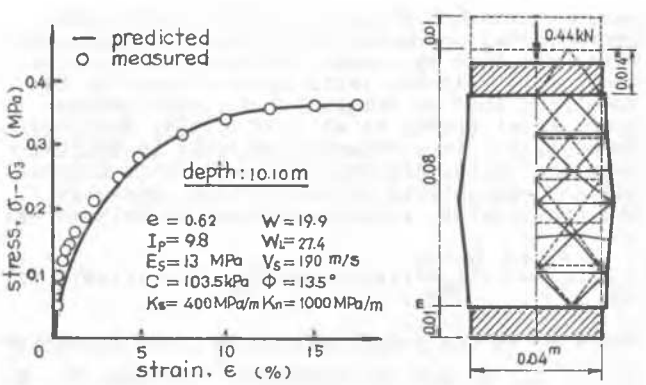

Figure 5. Analysis of triaxial compression test

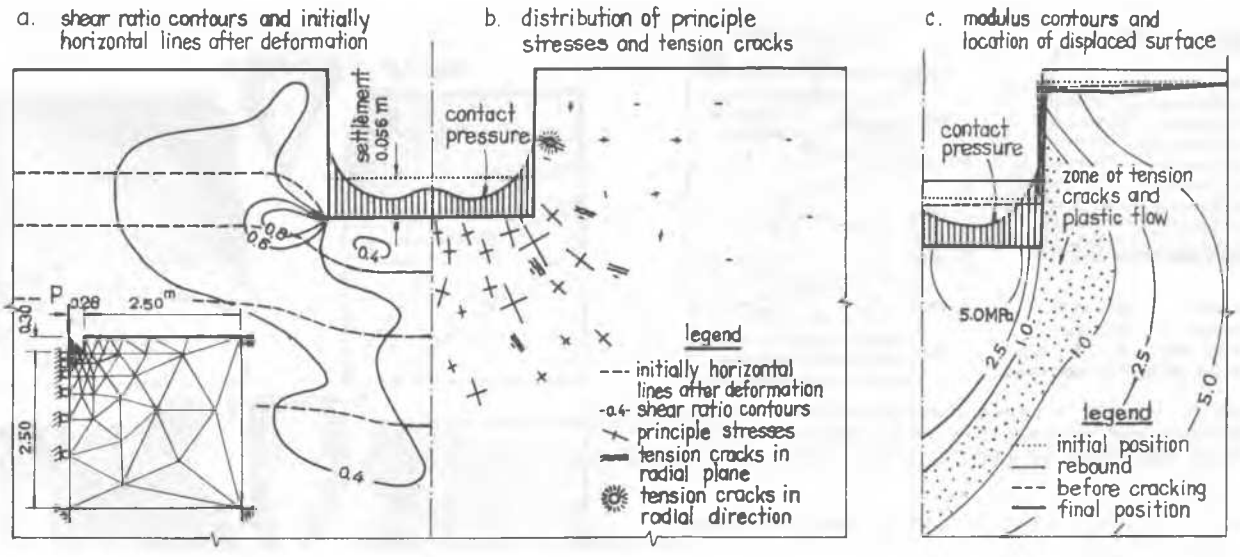

Figure 6. Results of an analysis of PLT on medium to dense saturated quaternary clay

In order to verify the applicability of the proposed method and to calibrate the parameters of the soil, a CIU triaxial compression test of the soil under the PLT is analysed with results as shown in Fig. 5. It may be seen from the figure that satisfactory accord between predicted and measured stress-strain behavior is obtained with reasonable soil parameters.

6 ANALYSIS OF A PLATE-LOAD TEST

The method is then applied to the analysis of a plate-load test on the same soil in a foundation pit 9.1 m deep on a round plate with a radius of 0.282m indented 0.30m from the bottom of the pit. The finite element configuration, the soil parameters adopted and the results of analysis are as shown in Fig. 6 and 7. The analysis begins with a release of load due to the excavation of the foundation pit followed by step-wise increases of loads on the plate up to 0.8 MPa with two rebound branchs. As may be seen from the figures, besides obtaining a predicted load-settlement curve that follows closely the measured readings, a hitherto unnoticed zone of tensile cracks and plastic flow is shown by the analysis to gradually appear beneath and around the loaded plate isolating a cone-shaped volume of soil under the plate which is believed to be the cause of the turning point and the subsequent steep and fairly straight tangent of the load-settlement curve. This brings to light a new form of tension induced failure quite different from the classic mode of shear failure derived from a rigid-plastic assumption.

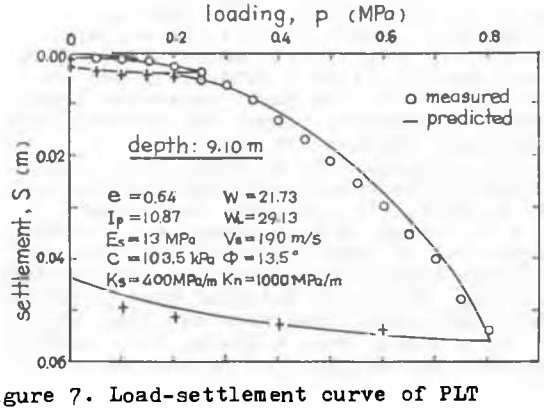

Figure 7. Load-settlement curve of PLT

7 ANALYSIS OF A CONE-PENETRATION TEST

A cone-penetration test on the same soil is analysed by prescribing 1/2 of the step-wise motion to the strain-controlled dynamic interface elements as shown in Fig.4b to simulate the gradual process of penetration per load-case. To take account of the remolding and lubricating effect of the penetration action on the saturated clay, the cohesion of the interface is taken as zero and the soil next to it is assumed to be reduced gradually to a state of fluid incapable of sustaining tensile and shearing stress with the relation between normal stress and strain expressed as:

$$\sigma_r = \sigma_z = \sigma_t = \frac{M_1}{3}(\epsilon_r + \epsilon_z + \epsilon_t) \qquad (6)$$

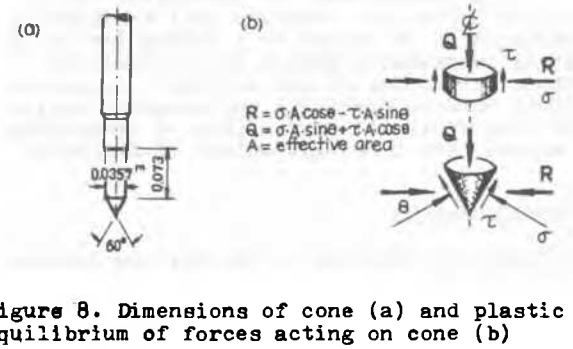

Figure 8. Dimensions of cone (a) and plastic equilibrium of forces acting on cone (b)

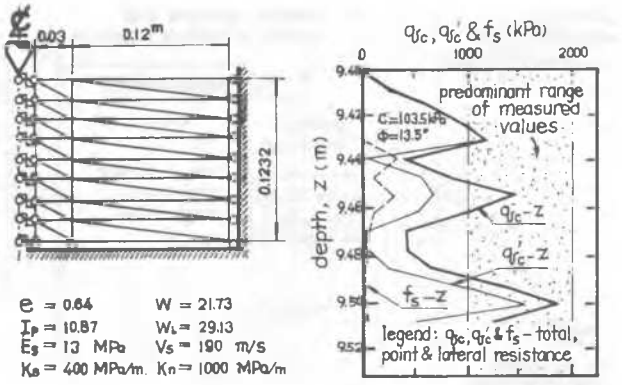

Figure 9. Finite element configuration, soil parameters and penetration resistance of a preliminary analysis of CPT

where σ_r, σ_z, σ_t, ϵ_r, ϵ_z, and ϵ_t are the normal stresses and strains in the r, z and t directions. The penetration resistance is obtained by summing up the vertical forces acting on the surface of the cone in plastic equilibrium divided by the horizontal area of the cone as shown in Fig. 8. A very simple finite element configuration is used for a preliminary analysis (Fig.9). A zigzag variation of penetration resistance with depth is obtained by the analysis in the soil with a uniform stress-strain-strength property as shown also in Fig. 9. The variations of deformation and modulus during penetration are as shown in Fig. 10. As may be seen from the figure, the lateral deformations also vary in a zigzag way which are caused by a succession of alternating compression/squeezing and tension/splitting action during penetration.

8 PRELIMINARY CONCLUSIONS

Although a great deal of work remains to be done, the following may be concluded from this preliminary study:

1. The pseudo-elastic model and the method of analysis proposed may be used to analyse the predominantly undrained stress-strain behavior of medium to dense quaternary soils during PLT and CPT.
2. A hitherto unnoticed cone-shaped volume of soil under the loaded plate surrounded and isolated by a tension-induced shear-belt is shown by the analysis to be the cause of the turning point and the subsequent steep and fairly straight tangent of the load-settlement curve of PLT.
3. A zigzag variation of penetration resistance with depth in a uniform soil is shown by the analysis to be caused by a succession of alternating compression/squeezing and tension/splitting action during penetration. A general agreement between predicted and measured resistances also shows the possibility of developing this method into a routine method of analysis.

9 ACKNOWLEDGEMENTS

The authors are indebted to the Beijing Geotechnical Institute and many colleagues for their valuable support which renders this work possible.

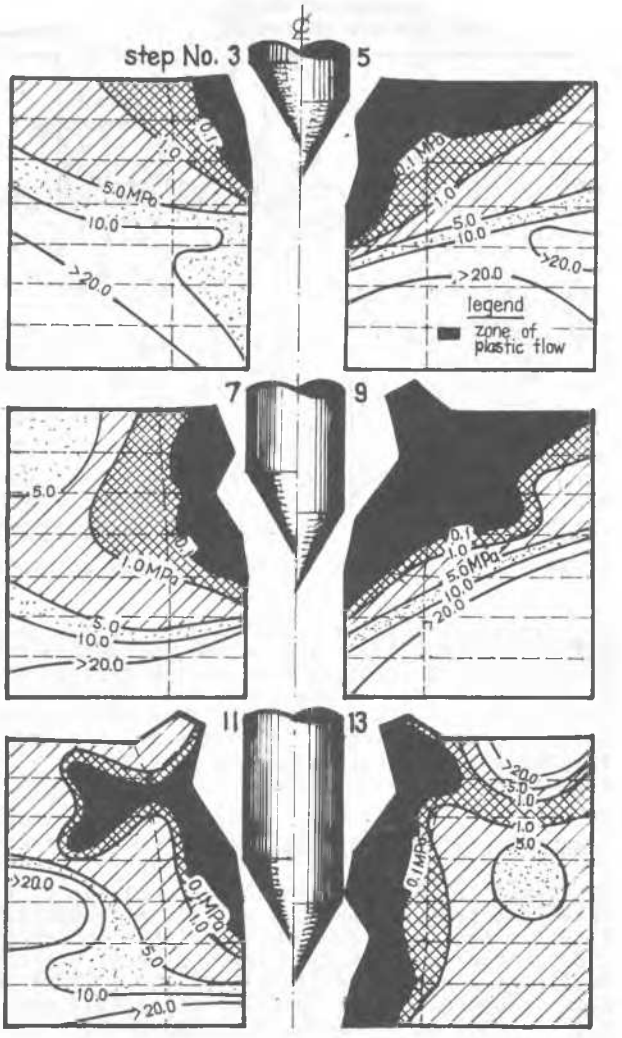

Fig. 10. Deformation and modulus contour of a preliminary analysis of CPT

10 REFERENCES

Andersen, K.H. & Per Stenhamar (1982). Static plate loading tests on overconsolidated clay. J.Geot.Eng.Div., ASCE, Vol.108, No.GT7, July.

Baligh, M.M. (1985). The strain path method. J. Geot.Eng.Div., ASCE, Vol.111, No.9, Sept.

Battaglio, M., Bruzzi, D., Jamiolkowski, M. & Lancellotta, R. (1986). Interpretation of CPT's and CPTU's, 1st part: undrained penetration of saturated clays. IV International Geotechnical Seminar, Singapore.

Zhang, G.X., Zhang, N.R. & Zhang, F.L. (1981). Nonlinear differential settlement analysis. Proc. XICSMFE, (2), 291-294, Stockholm.

Zhang, G.X., Zhang, N.R. & Zhang, F.L. (1984). A comparison of some predicted and observed settlement behaviours of Box-type foundations in Beijing. Proc. 3rd International Conference on Tall Buildings, Hong Kong and Guan Zhou.

Zhang, G.X., Zhang, N.R. & Zhang, F.L. (1985). Experiment and analysis of pressuremeter mechanism. Proc. XIICSMFE, (2), 959, San Francisco.